

Search for LBV Candidates in the M 33 Galaxy

A.F. Valeev, O. Sholukhova, and S. Fabrika

Special Astrophysical Observatory, Nizhniy Arkhyz 369167, Russia
E-mail: azamat@sao.ru, olga@sao.ru, fabrika@sao.ru

June 6, 2018

ABSTRACT

A total of 185 luminous blue variable star (LBV) candidates with $V < 18^m.5$ are selected based on the results of aperture photometry. The primary selection criterion is that the prospective candidate should be a blue star with $H\alpha$ emission. In order not to overlook appreciably reddened LBV candidates, we compose an additional list of 25 red ($0^m.35 < B - V < 1^m.2$, $V < 18^m.5$) emission star candidates. A comparison with the list of known variables in the M 33 galaxy showed 29% of our selected candidates to be photometrically variable. We also find our list to agree well with the lists of emission-line objects obtained in earlier papers using different methods.

1 INTRODUCTION

Luminous blue variables are the most massive stars during the final stage of evolution [[Humphreys & Davidson (1994)]. It is a rather short-lived stage characterized by high mass-loss rate and mass ejections into the interstellar medium during outbursts. The bolometric luminosities of such stars are close to the Eddington limit, below which radiation pressure can still be balanced by gravity forces.

Modern model computations often involve explicitly preset time of the beginning of the LBV evolution and the duration of this stage (see, e.g., [Meynet et al. (2007)]), because these parameters are impossible to infer via self-consistent modeling. The input parameters in these cases are based on the most recent observational data. Modeling is further complicated due to the lack of a consensus concerning the evolutionary sequence of massive stars – e.g., even the LBV \rightarrow WR transition remains an open issue ([Smith & Owocki (2006)], [Smith & Conti (2008)], [Smith (2008)]). The number of known LBV stars in our Galaxy is too small to test the agreement between the model tracks and observational data.

The number of known and well-studied massive stars at the final stages of evolution — LBV stars, WR stars, B[e]-type supergiants, and supergiants and hypergiants with various temperatures — should be increased considerably. These objects have very different observational manifestations. Only with a sufficient number of stars with known parameters it will be possible to reliably identify the results of modeling of the evolution of massive stars with observed objects. On the other hand, a considerably increased sample will make the interpretation of model computations more reliable. The discovery and study of new massive stars at the final stages of evolution (hereafter referred to as “LBV-like” stars) would lay down the necessary basis for linking theory with observation so that the studies of LBV stars will no longer remain mostly descriptive.

The main goal of this paper is to search for and identify LBV candidates. In the Milky Way such objects

are hidden by strong interstellar extinction in the Galactic disk. They are currently discovered in IR sky surveys (e.g., [Gvaramadze et al. (2009)]). Its fortunate orientation and sufficiently large population of early-type stars makes the M 33 galaxy of the Local Group an ideal object to be searched for LBV-like stars [Ivanov et al. (1993)]. Here we adopt an M 33 distance modulus of $24^m.9$ (e.g., [Bonanos et al. (2006)]), which corresponds to a distance of 950 kpc.

In their review, Humphreys and Davidson [Humphreys & Davidson (1994)] summarize all the data known about LBV stars by that time: their list of confirmed LBV stars in M 33 included Var B, Var C, Var 2, and Var 83, and V 532 (GR 290, the “Romano star” [Romano (1978)]) was considered to be an LBV candidate. Later, the latter had its LBV status confirmed both spectroscopically [Fabrika (2000)] and photometrically [Kurtev et al. (2001)]. It was studied in more detail by Fabrika et al. [Fabrika et al. (2005)] and Viotti et al. [Viotti et al. (2006, 2007)]. The star Var A in M 33 is now commonly classified as a cool hypergiant [Humphreys et al. (1987)], [Humphreys et al. (2006)], [Viotti et al. (2006)]. Although this object exhibits all the features characteristic for LBV stars — it suddenly brightened in 1950–1953 [Hubble & Sandage (1953)] to become one of the most luminous stars in M 33 with a spectral type F — its current spectral type (M) is untypical for classical LBV stars. However, given the fewness of LBV stars hitherto studied, it is possible that the known classical LBV states [Humphreys & Davidson (1994)] do not cover all possible properties of these objects. The Var A star meets the criteria of LBV class both in terms of luminosity (mass) and photometric variability [Valeev et al. (2009)].

Spectroscopic observations of LBV-like star candidates from our list allowed us to discover a new (the seventh) LBV star N93351 in the M 33 galaxy [Valeev et al. (2009)]. We use very limited archival data to construct the light curve of the star and find it to be variable with the light variations of about $0^m.4$ a year. Further observations of N93351 both

photometric and spectroscopic are needed to confirm the evolutionary status of the star.

Various groups of authors [Neese et al. (1991)], [Spiller (1992)], [Calzetti et al. (1995)], [Fabrika & Sholukhova (1995)], [Massey et al. (1996)], [Sholukhova et al. (1997)], [Sholukhova & Fabrika (2000)], [Corral & Herrero (2003)] used various methods to search for LBV stars in M33. The principal method consists in searching for $H\alpha$ sources coincident with early-type stars. Although LBV stars need not inevitably be blue objects [Sterken et al. (2008)], many authors targeted their search on early-type stars. Some authors looked for SS 443-like objects [Neese et al. (1991)], [Calzetti et al. (1995)], [Fabrika & Sholukhova (1995)]. The spectrum of SS 433 resembles those of late WR stars [Fabrika (2004)].

The team of Massey et al. [Massey et al. (2006)] made a new step toward the study of the massive stellar population of the M33 galaxy. The above authors used CCD images of the galaxy to produce a catalog of 146622 stars down to a limiting magnitude of 23 containing broad-band photometric measurements with an accuracy of 1–2%. In their next paper [Massey et al. (2007)], the team reported a list of emission stars in Local Group galaxies including M33. The main purpose of this study was to find new LBV star candidates. To this end, the above authors adopted the following criteria: a constraint on the $H\alpha$ line flux; $H\alpha$ line flux had to be greater than the [SII] line flux; the [OIII] line flux had to exceed the continuum flux, and a constraint was imposed on the star’s color (see [Massey et al. (2007)] for details). Massey et al. [Massey et al. (2007)] report 37 LBV stars and LBV candidates in M33. Some of the candidates reported by Massey et al. [Massey et al. (2007)] have been identified before [Corral (1996)], [Sholukhova et al. (1997)], [Fabrika & Sholukhova (1995)], [Sholukhova & Fabrika (2000)], [Fabrika (2000)].

We performed independent aperture photometry of bright objects with $V < 18^m.5$ in all filters (UBVRI and $H\alpha$) on the CCD frames of Massey et al. [Massey et al. (2006)]. We used the same methods to select LBV candidates as Fabrika et al. [Fabrika & Sholukhova (1999a)]. Emission-line objects are easily identifiable on the “ $H\alpha$ -line flux vs. V-band flux” diagram, because they lie above the linear relation outlined by objects without the $H\alpha$ emission (see below for details).

As a result of this work we composed a list of blue LBV-like star candidates in M33. In order not to overlook highly reddened objects we composed an additional list of red $H\alpha$ emission objects selected with less stringent color criteria.

2 OBSERVATIONAL DATA

We downloaded from the NOAO science archive (<http://www.archive.noao.edu/nsa/>) all primarily reduced M33 frames taken by Massey et al. [Massey et al. (2006)] with the coordinate grid applied. Observations were made in October 2000 and September 2001 with the the 4-m telescopes of the KPNO and CTIO telescopes using UBVRI filters and narrow-band (50 Å) $H\alpha$. The UBVRI and $H\alpha$ -filter images were taken during photometric nights when the seeing was 0'6 to 0'8, and 0'8 to 1'0, respectively. The detector employed was a mosaic of eight 2048×4096

CCDs. Each image has a field of view of 36'×36' and a scale of 0'26/pix (after primary reduction and distortion correction). The M33 galaxy was subdivided into three zones with each zone observed five times with a small offset to fill the gaps between the CCDs in the mosaic. In this paper we use 15 mosaic images in each filter. A more detailed description of the data and primary reduction steps can be found in [Massey et al. (2006)].

3 APERTURE PHOTOMETRY

Our aim was to select stars with $H\alpha$ emission — the LBV candidates. The $H\alpha$ images contain both point and extended objects and therefore in the process of photometry we must check that measurements in different filters refer to the same object. This condition should be satisfied even in crowded fields and in complex $H\alpha$ regions, something that is difficult to achieve in automatic photometry of several hundred thousand objects [Massey et al. (2007)].

Aperture photometry has an important advantage over PSF photometry in that it makes it possible to determine the flux from an object without making any assumptions about its structure and the form and parameters of the point-spread function (PSF) in the Earth atmosphere. The use of the averaged PSF may introduce an error in the estimated flux due to the variation of the form of the PSF across the field. A problem with aperture photometry in crowded fields is that the aperture radius should be chosen individually for each object so as to keep all other objects outside the aperture. The determination and application of aperture correction is yet another problem to be faced when performing aperture photometry. However, if we need not determine the total flux, but only the flux difference in different filters, the same aperture size can be used in all filters. It is also important that seeing is approximately the same in all filters. The observations of Massey et al. [Massey et al. (2006)] meet this condition.

We used standard IRAF¹ tools for photometric measurements and all performed auxiliary operations in the batch mode using programs written in Python language.

To choose the optimum aperture size, we performed the photometry of each object varying the aperture radius R from 0'5 to 6'0 with a step of 0'25. We estimated the background level using the median averaging over a ring with the inner and outer radii equal to R and $R+\Delta R$, respectively, where $\Delta R = 2''$. In this approach the flux from a single object first smoothly increases with increasing radius R and then remains approximately constant (the plateau in Fig. 1a). The vertical coordinate of the point where the plateau begins corresponds to the full flux from the star in the filter considered. After reaching the plateau the flux becomes practically ceases to vary with aperture radius, whereas the dependence is very strong when the radius approaches the plateau. We consider the optimum radius of the object to be equal to $R_{0.9}$, the abscissa of the point corresponding to 90% of the total flux. We interpolate the

¹ IRAF is distributed by the National Optical Astronomy Observatory, which is operated by the Association of Universities for Research in Astronomy (AURA) under cooperative agreement with the National Science Foundation.

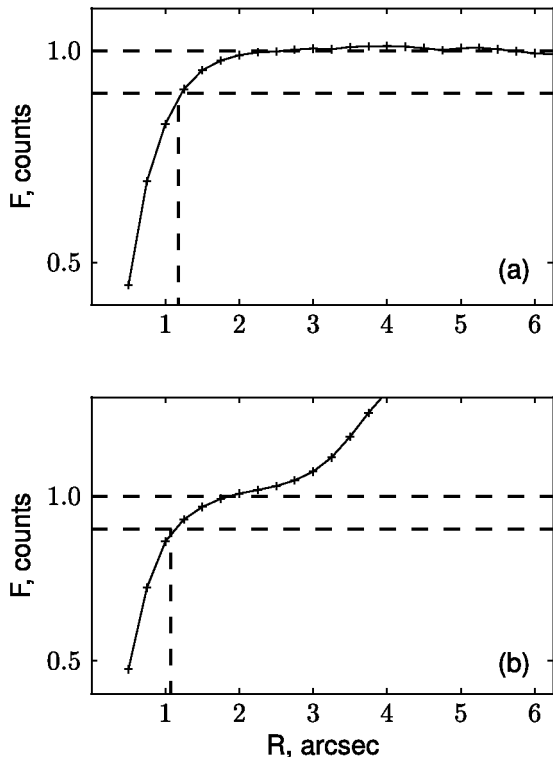


Figure 1. Examples of typical variations of normalized stellar fluxes as a function of the aperture radius in two cases: the photometry of an isolated object (a) and the photometry of an object with a close neighbor (b). The crosses correspond to the results of measurements. The horizontal lines are drawn at the levels corresponding to 0.9 and 1.0 total flux. The vertical line indicates the radius of the aperture corresponding to 0.9 of the total flux. In panel (b) the flux continues to increase after reaching the plateau because of the contribution from the neighboring object.

curve by drawing a cubic spline through the measured data points.

In the presence of a nearby neighboring object (see Fig. 1b) the flux continues to increase even after reaching the plateau. We chose the flux and optimum aperture radius to be same for all filters at the supposed location of the plateau so as to keep the flux from the neighboring objects outside the measurement aperture.

In the case of a two-dimensional Gaussian 90% of the total flux corresponds to $R_{0.9} = 1.95\sigma$, where σ is the parameter of the Gaussian. The full width at half maximum (FWHM) of a two-dimensional Gaussian (which, by definition, corresponds to the size of a point source) is reached at the aperture radius of $R_{FWHM} = 1.18\sigma$. Hence given the observed $0''.6-0''.8$ seeing, we can expect the sizes of point-source images on the CCD to be, according to our definition, $R_{0.9} = 1''.0 - 1''.3$.

To determine the optimum aperture R (or the size of the object), we compute the mean $R_{0.9}$ values averaged over the four broad-band filters. We then measure the flux in the narrow-band $H\alpha$ filter within the same $R_{0.9}$ aperture and divide it by 0.9 to compute the total flux. The resulting quantity is equal to the total flux if we are dealing with a point source in the $H\alpha$ filter. In the case of an extended object in the $H\alpha$ filter (e.g., an HII region), the inferred

quantity is an estimate of the total flux from the part of the extended source, where the point source was measured in the broad-band filters.

Hence we use the $R_{0.9}$ quantity to measure the size of the source and use the count at the plateau level to estimate the fluxes in filters as shown in Fig. 1.

The image of the galaxy consists of several zones with each zone observed several times with different offsets so that many objects are measured repeatedly in each particular filter. We corrected each measurement for airmass by multiplying it by $1/\cos z$, where z is the zenith angle. To construct the mean dependence of flux on the aperture radius, we computed the median of the dependences based on individual measurements. Individual dependences differ mostly because of night-to-night seeing variations. Averaging showed that the results of individual measurements of the same object do not differ by more than 7–10%, which is acceptable accuracy for our purposes of object selection.

Massey et al. [Massey et al. (2006)] demonstrated that each CCD frame of the mosaic image should be reduced separately because of considerable differences between the detector parameters (gain, read-out noise, and spectral sensitivity). We therefore partitioned each composite image into eight individual frames corresponding to different detectors and reduced each frame separately.

Our task of extracting objects with excess flux in the $H\alpha$ filter does not require the determination of calibrated fluxes, and we therefore selected objects based on instrumental fluxes exclusively. Only at the final stage of our work we converted instrumental fluxes into magnitudes using the following averaged calibrating coefficients:

$$m_U = -2.5 \log(F_U) + 30.20$$

$$m_B = -2.5 \log(F_B) + 29.43$$

$$m_V = -2.5 \log(F_V) + 29.61$$

$$m_R = -2.5 \log(F_R) + 29.84$$

$$m_{H\alpha} = -2.5 \log(2 \times 10^{-16} \times F_{H\alpha}/300),$$

where F is the flux from the object measured during the exposure time in the instrumental system in the corresponding filter. We determined the averaged calibrating coefficients by performing the photometry of single stars and comparing their instrumental magnitudes with the magnitudes reported in the catalog of Massey et al. [Massey et al. (2006)], and only adopted the $H\alpha$ calibration from [Massey et al. (2007)]. Note once again that our main task requires no flux calibration.

4 SELECTION OF LBV-LIKE CANDIDATE OBJECTS

For our photometric measurements we selected a total of 2304 objects with $V < 18^m.5$ from the catalog of Massey et al. [Massey et al. (2006)]. We adopt an average interstellar extinction of $A_V \approx 1^m.0$ for the brightest stars in the M33 galaxy (e.g., [Fabrika & Sholukhova (1999b)] $A_V \approx 0^m.95 \pm 0^m.05$), and an M33 distance modulus

of 24^m9 [Bonanos et al. (2006)]. Given our adopted criteria ($V < 18^m5$ and $(B - V) < 0^m35$) the main list includes stars with $M_V < -7^m4$ and $(B - V)_0 \leq 0^m0$. It includes all bright supergiants of luminosity class Iab and more luminous stars, as well as the hottest supergiants (with B0-type and earlier spectra) of luminosity class Ib [Allen (1977)]. Hence our final list should include all potential LBV star candidates.

In the case of the photometry of close groups consisting of two or more objects, where the plateau in the “aperture radius–flux” dependence for all broad-band filter images can be reached at apertures greater than the aperture of a point source, we treated such a close group as a single object. It is evident that some of such “single” objects will prove to be groups of stars if observed with a better spatial resolution. In our photometric measurements a close group could consist of several objects from the initial catalog of Massey et al. [Massey et al. (2006)]. We attributed the resulting measurement to one of the objects of the initial catalog and did not perform the photometry of other members of the group. If one of the objects in such a close group is an $H\alpha$ emission star the entire group shows excess flux in the $H\alpha$ filter.

We were able to perform the photometry of 2075 objects. Photometric measurements were impossible to perform for the remaining 229 objects, because they were located at the boundary of the galaxy, showed no plateau on the “aperture radius–flux” dependence, or were members of one of the close groups.

After the photometric reduction we selected the emission-line candidates using the method described by Fabrika et al. [Fabrika & Sholukhova (1999a)]. To this end, we constructed the $V-H\alpha$ diagram, where most of the objects lie within a broad band of a linear relation (Fig. 2). Emission-line objects lie above this relation because of the appreciable excess of their $H\alpha$ fluxes relative to the remaining, nonemission part of the sample. Figure 2 shows an example of the $V-H\alpha$ relation.

It is evident that this linear “main sequence” is due to the fact that stars that are brighter in the V band are also relatively brighter in the $H\alpha$ band. This “main sequence” is rather broad due both to absorption stars and to spectral peculiarities of stars of different temperatures. However, it is a well-defined sequence.

At the next stage we used only 707 stars with $B - V < 0^m35$ out of the entire sample of 2075 objects. We show these 707 stars in Fig. 2. The $V-H\alpha$ diagram for the entire sample including both red and blue stars would consist of two partially overlapping parallel sequences: the red stars in M33 and in Milky Way.

We used the following technique to select emission-line stars on the $V-H\alpha$ diagram. We first fitted a linear relation to all points of the sample in order to determine the main sequence of nonemission stars, and then computed the r.m.s. deviation (hereafter referred to as σ) of data points from this linear relation. At the next stage we discarded the objects with the $H\alpha$ excess greater than 2.5σ ; fitted a new relation, and computed the new σ value based on the remaining data points. We computed the final σ for the rectified sequence obtained after seven to eight iterations when the number of stars ceased to change.

We then choose the minimum excess such that objects lying above it should be considered to be emission-line stars. We found that the $H\alpha7$ object with an $H\alpha$ emission-line

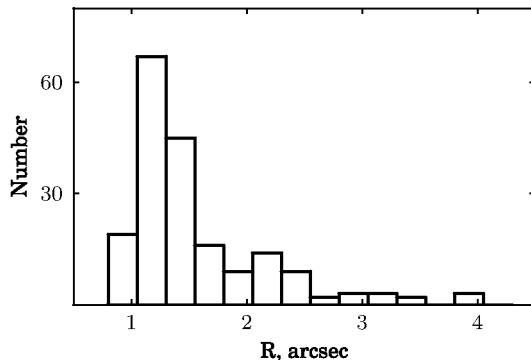


Figure 4. Histogram of the $R_{0.9}$ sizes of our selected objects (Table 1). The maximum of this distribution, which is located at $1''0-1''3$, corresponds to the expected size of point sources (see Section 3). Sources with greater sizes correspond to groups, which we treated as single objects in our photometric measurements.

equivalent width of 3\AA [Sholukhova et al. (1997)] lies 1.01σ above the main relation (number 018246). We therefore decided that emission objects should lie about 1.0σ above the main sequence and used this criterion to select 185 objects, which we list in Table 1.

The first three columns of Table 1 list the number of the object and its J2000.0 coordinates according to the catalog of Massey et al. [Massey et al. (2006)]. The next columns give our measured V -band magnitude and the $(B - V)$ color index; the excess “s” above the main sequence in the units of σ (used as the estimate of the intensity of the hypothetical $H\alpha$ emission), and R , the aperture size $R_{0.9}$ averaged over all four broad-band filters (in arcseconds). The complete version of the table is available at <http://jet.sao.ru/~azamat/LBVsearch/ /blue.dat>.

Given that red stars with $(B - V) \geq 0^m35$ can also be LBV candidates (e.g., the highly reddened η Car), we selected from our list the candidate emission-line objects among other stars with $V < 18^m5$. We then used the method described above to compute the r.m.s. deviation σ of the $(B - V) - (R - H\alpha)$ diagram for objects with $(B - V) \geq 0^m35$ shown in Fig. 3. We included into the list of LBV candidates (Table 2) only the objects with the excess of the $(R - H\alpha)$ color excess greater than 2σ above the main sequence of stars with $(B - V) \geq 0^m35$.

We imposed an additional constraint $(B - V) < 1^m2$ on the colors of red stars in Table 2. Note that no objects with $H\alpha$ excess were selected in the $(B - V) = 1^m2 - 1^m3$ interval. Given the known properties of LBV stars [Humphreys & Davidson (1994)] it can be concluded that their photospheric temperatures cannot be lower than 7000K, which corresponds to $(B - V)_0 \approx 0^m25$. The observed color of such a star should be $(B - V) \approx 1^m2$ even if the interstellar extinction toward it were as high as $A_V = 3^m0$. Moreover, the spectra of stars with $(B - V)_0 > 1^m3$ exhibit TiO absorption bands, which may mimic $H\alpha$ emission. In view of these considerations, our constraint $(B - V) < 1^m2$ appears to be quite reasonable.

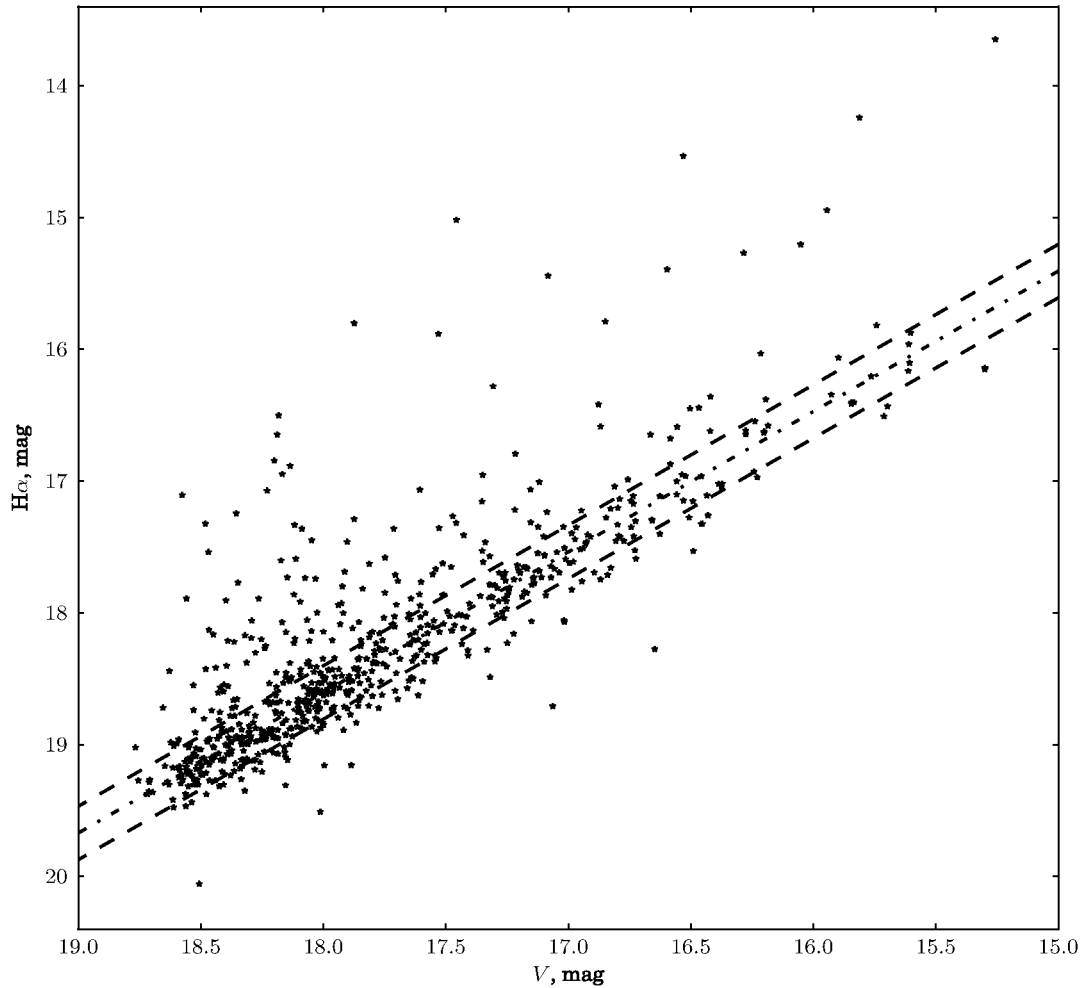


Figure 2. $H\alpha$ -band versus V -band magnitude diagram for 707 objects with $B - V < 0.35$. The dashed-and-dotted line shows the relation for the nonemission sample. The dotted lines show the $\pm 1\sigma$ levels. Objects located above 1σ level are listed in Table 1 as emission-line objects.

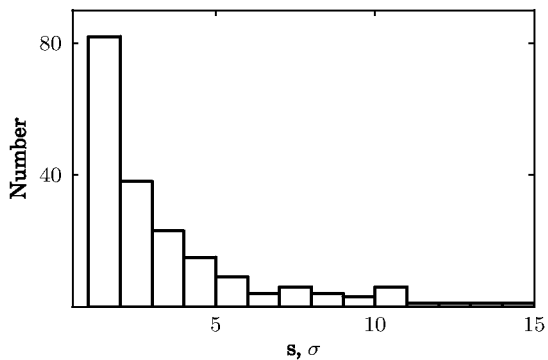


Figure 5. Histogram of the $H\alpha$ flux excess above the main sequence for nonemission stars in the units of σ (Table 1).

5 COMPARISON WITH OTHER CATALOGS

We cross-correlated the coordinates of objects of our list of blue candidate emission-line stars with other published lists. To this end, we used TOPCAT² program, running the standard identification algorithm where objects from the first catalog are selected that are located inside the ε -neighborhood of an object of the second catalog. We set the

² TOPCAT was initially (2003-2005) developed under the UK Starlink project (1980-2005, R.I.P.). From July 2005 until June 2006, it was supported by grant PP/D002486/1 from the UK's Particle Physics and Astronomy Research Council. Maintenance and development has been funded from July 2006 until December 2007 by the European VOTech project within the UK's AstroGrid, and directly from AstroGrid funding beyond that.

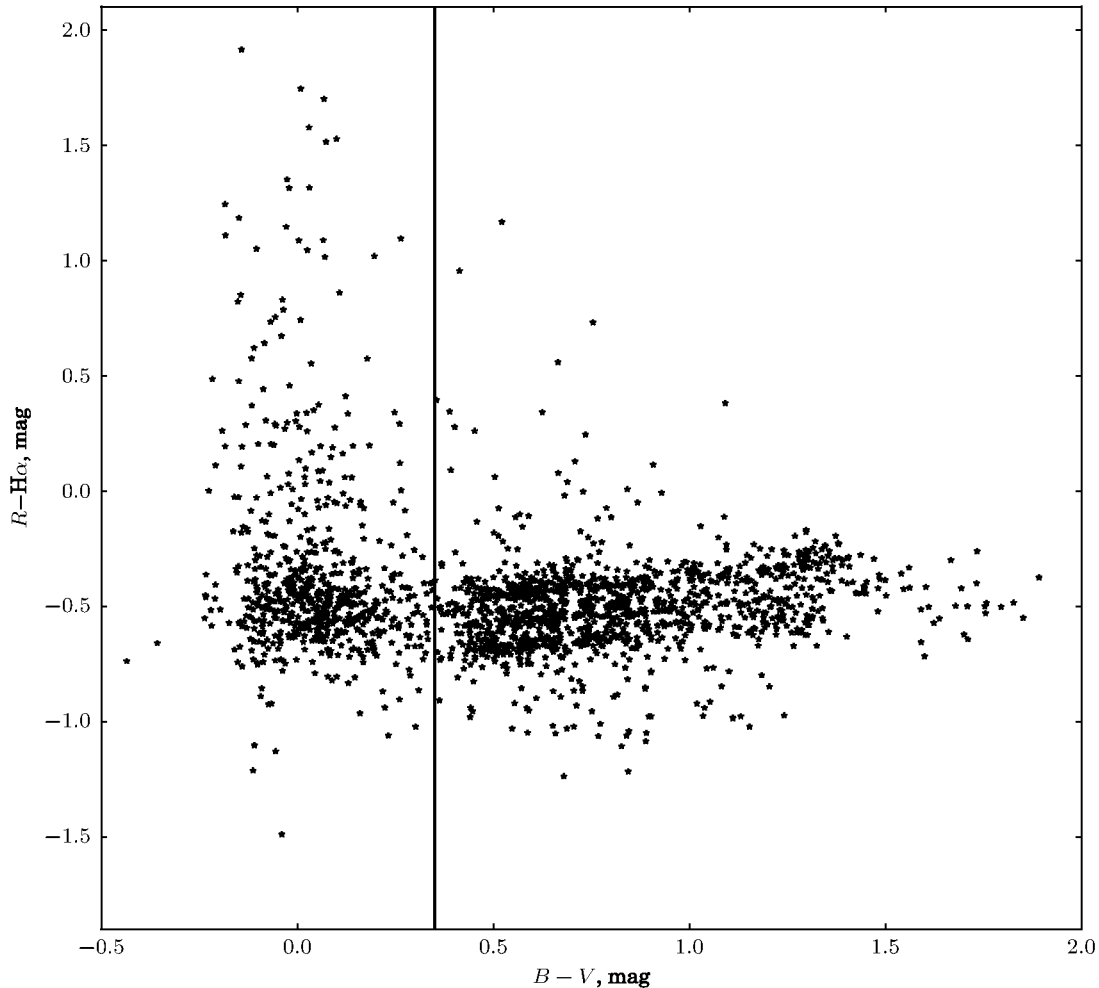


Figure 3. Results of the photometry of all the 2075 sample objects with $V < 18^m5$. Objects with $B - V < 0^m35$ in the top left part of the figure were investigated based on the criterion illustrated in Fig. 2. Objects in the top right part of the figure with an $R - H\alpha$ color excess are listed in Table 2 as potential LBV candidates with strong interstellar extinction.

radius of ε -neighborhood (or the “error box”) individually for each pair of catalogs.

The cross-correlation with the lists of sources detected by Chandra [Grimm et al. (2005)] and XMM Newton [Pietsch et al. (2004)] X-ray telescopes with $5''0$ -large error boxes yielded one identification. This X-ray object (the supernova remnant SNR B013059+30177 [Gordon et al. (1998)]) has already certain optical identification and is located near the N085197 (J013348.03+303304.8) object from Table 1. A cross-correlation with the list of ultraviolet sources [Massey et al. (1996)](UIT) yielded 23 identifications within $3''0$ -large error boxes, of which only four objects have not yet been spectrally classified.

Classical LBV stars are characterized by irregular light variations on various time scales, and therefore we cross-correlated our list with the catalog of variable stars in M 33 [Hartman et al. (2006)], which contains more than 36000

variables down to a limiting magnitude of $V \approx 24^m0$ with the coordinates accurate to $0''.2$. We found 54 stars in common, which makes up for 29% of our complete list of blue objects with $H\alpha$ emission.

We also cross-correlated our list with two lists of emission-line objects composed in different years [Massey et al. (2007)], [Fabrika & Sholukhova (1999a)]. The evident criterion based on the exact coincidence of the coordinates in our list with those of LBV candidates selected by Massey et al. [Massey et al. (2007)] yielded 113 stars in common, whereas the cross-correlation with the catalog of Fabrika et al. [Fabrika & Sholukhova (1999a)] with a $2''0$ -large error box yielded 50 identifications.

6 DISCUSSION

Figure 4 shows the size distribution of 185 selected blue emission-line objects from Table 1. The maximum of the distribution is near $1''.0$ – $1''.3$, which corresponds to the value expected for point objects observed with a seeing of $0''.6$ – $0''.8$ (see Section 3). Sources with greater sizes correspond to groups of objects.

Figure 5 shows the distribution of the flux excess “s” in the $H\alpha$ filter for selected blue objects above the main linear relation for nonemission objects. As is evident from the figure, the number of objects continuously decreases with increasing $H\alpha$ -line flux excess.

Note that Table 1 contains no objects in the $V \approx 14^m.0$ – $15^m.5$ magnitude interval. This means that seven objects with $V < 14^m.0$ must be foreground stars of the Milky Way, although, only spectroscopic observations can explain the excess of $H\alpha$ -line fluxes of these objects. A 62% overlap between our list of blue objects and the list of emission-line objects of [Massey et al. (2007)] shows that both criteria can be used to select LBV candidates. Non cross-identified objects of both lists also deserve a special investigation in order to understand what subclass of emission-line objects is rejected by each method.

We included into our additional list of LBV candidates (Table 2) only objects with $V > 16^m.0$, because no red objects were selected in the $V \approx 15^m.0$ – $16^m.0$ magnitude interval, and brighter stars are definitively foreground objects. The fact that two red emission objects (N006862 and N141751) are also included in the catalog of Massey et al. [Massey et al. (2007)], where they are classified as hot LBV candidates, corroborates the need for the search for reddened stars.

We perform spectroscopic observations of blue emission objects with the 6-m telescope of the Special Astrophysical Observatory of the Russian Academy of Sciences. We already found [Valeev et al. (2009)] the star N93351 whose spectrum exhibits broad hydrogen emissions and numerous FeII and [FeII] emission features. We constructed the spectral energy distribution for this star in the wavelength interval 3000–80000Å and showed that this object, like Var A, has a strong infrared excess. The results of our analysis led us to conclude [Valeev et al. (2009)] that N93351 should be classified as an LBV-type star.

7 CONCLUSIONS

We used archive of UBVR and $H\alpha$ -band CCD images of the M33 galaxy to perform aperture photometry of all objects from catalog [Massey et al. (2006)] with $V < 18^m.5$. We selected LBV candidate stars in M33 using a criterion based on the excess of the $H\alpha$ -line flux over the V -band flux. We selected a total of 185 emission-line candidates — blue stars with $(B - V) < 0^m.35$.

Variability on different time scales is a classical property of LBV stars and therefore we cross-correlated our list with the catalog of variable stars in M33 [Hartman et al. (2006)] to find that 29% of our blue candidates exhibit light variations. Part of LBV stars are hot and should be studied in the ultraviolet. A cross-correlation with the list of

ultraviolet sources showed that 23 LBV candidates were indeed detected by the UIT space telescope [Massey et al. (1996)]. Our list of blue emission-line candidates overlaps by 27% with the list of Fabrika et al. [Fabrika & Sholukhova (1999a)] based on photometric images and simple criteria. Our list also overlaps by 62% with the list of LBV candidates [Massey et al. (2007)] based on the same observational material, but subject to more complex criteria of the selection of LBV candidates.

LBV stars may be appreciably, and sometimes rather strongly, reddened. We therefore composed an additional list of 25 red stars with $0^m.35 < B - V < 1^m.2$ selected using the criterion of the excess of the $R - H\alpha$ color. These objects may be reddened LBV stars.

We thus report our complete list of LBV candidates in M33 down to a V -band limiting magnitude of $18^m.5$. To perform a detailed classification of the stars of our catalog, we observe them spectroscopically with the 6-m telescope of the Special Astrophysical Observatory of the Russian Academy of Sciences. We will publish the results of these spectroscopic observations in our next papers.

ACKNOWLEDGMENTS

This work was supported by the Russian Foundation for Basic Research (project nos 09-02-00163 and 07-02-00909).

References

- Bonanos A. Z., Stanek K. Z., Kudritzki R. P., Macri L. M., Sasselov D. D., Kaluzny J., Stetson P. B., Bersier D., Bresolin F., Matheson T., Mochejska B. J., Przybilla N., Szentgyorgyi A. H., Tonry J., Torres G., 2006, *Astrophys. J.*, 652, 313
- Calzetti D., Kinney A. L., Ford H., Doggett J., Long K. S., 1995, *Astronom. J.*, 110, 2739
- Corral L. J., 1996, *Astronom. J.*, 112, 1450
- Corral L. J., Herrero A., 2003, in J. M. Rodriguez Espinoza, F. Garzon Lopez, & V. Melo Martin ed., *Revista Mexicana de Astronomia y Astrofisica Conference Series Vol. 16 of Revista Mexicana de Astronomia y Astrofisica Conference Series, Luminous Blue Variables in the local universe.* pp 265–266
- Fabrika S., 2000, in H. Lamers & A. Sagar ed., *Thermal and Ionization Aspects of Flows from Hot Stars Vol. 204 of Astronomical Society of the Pacific Conference Series*, New LBV-like stars in M33. pp 57–+
- Fabrika S., 2004, *Astrophysics and Space Physics Reviews*, 12, 1
- Fabrika S., Sholukhova O., 1995, *Astrophys. and Space Sci.*, 226, 229
- Fabrika S., Sholukhova O., 1999a, *Astronom. and Astrophys. Suppl.*, 140, 309
- Fabrika S., Sholukhova O., 1999b, *Astronom. and Astrophys. Suppl.*, 140, 309
- Fabrika S., Sholukhova O., Becker T., Afanasiev V., Roth M., Sanchez S. F., 2005, *Astronom. and Astrophys.*, 437, 217

- Gordon S. M., Kirshner R. P., Long K. S., Blair W. P., Duric N., Smith R. C., 1998, *Astrophys. J. Suppl.*, 117, 89
- Grimm H., McDowell J., Zezas A., Kim D., Fabbiano G., 2005, *Astrophys. J. Suppl.*, 161, 271
- Gvaramadze V. V., Kniazev A. Y., Fabrika S., 2009, ArXiv e-prints
- Hartman J. D., Bersier D., Stanek K. Z., Beaulieu J., Kaluzny J., Marquette J., Stetson P. B., Schwarzenberg-Czerny A., 2006, *Monthly Notices Roy. Astronom. Soc.*, 371, 1405
- Hubble E., Sandage A., 1953, *Astrophys. J.*, 118, 353
- Humphreys R. M., Davidson K., 1994, *Publ. Astronom. Soc. Pacific*, 106, 1025
- Humphreys R. M., Jones T. J., Gehrz R. D., 1987, *Astronom. J.*, 94, 315
- Humphreys R. M., Jones T. J., Polonski E., Koppelman M., Helton A., McQuinn K., Gehrz R. D., Woodward C. E., Wagner R. M., Gordon K., Hinz J., Willner S. P., 2006, *Astronom. J.*, 131, 2105
- Ivanov G. R., Freedman W. L., Madore B. F., 1993, *Astrophys. J. Suppl.*, 89, 85
- Kurtev R., Sholukhova O., Borissova J., Georgiev L., 2001, *Revista Mexicana de Astronomia y Astrofisica*, 37, 57
- Massey P., Bianchi L., Hutchings J. B., Stecher T. P., 1996, *Astrophys. J.*, 469, 629
- Massey P., McNeill R. T., Olsen K. A. G., Hodge P. W., Blaha C., Jacoby G. H., Smith R. C., Strong S. B., 2007, *Astronom. J.*, 134, 2474
- Massey P., Olsen K. A. G., Hodge P. W., Strong S. B., Jacoby G. H., Schlingman W., Smith R. C., 2006, *Astronom. J.*, 131, 2478
- Meynet G., Eggenberger P., Maeder A., 2007, in A. Vazdekis & R. F. Peletier ed., *IAU Symposium Vol. 241 of IAU Symposium, Populations of massive stars in galaxies, implications for the stellar evolution theory*. pp 13–22
- Neese C. L., Armandroff T. E., Massey P., 1991, in K. A. van der Hucht & B. Hidayat ed., *Wolf-Rayet Stars and Interrelations with Other Massive Stars in Galaxies Vol. 143 of IAU Symposium, H α Emission-Line Stars in M33*. pp 651–+
- Pietsch W., Misanovic Z., Haberl F., Hatzidimitriou D., Ehle M., Trinchieri G., 2004, *Astronom. and Astrophys.*, 426, 11
- Romano G., 1978, *Astronom. and Astrophys.*, 67, 291
- Sholukhova O., Fabrika S., 2000, in D. Alloin, K. Olsen, & G. Galaz ed., *Stars, Gas and Dust in Galaxies: Exploring the Links Vol. 221 of Astronomical Society of the Pacific Conference Series, New LBV-like Stars in M33*. pp 171–+
- Sholukhova O. N., Fabrika S. N., Vlasjuk V. V., Burenkov A. N., 1997, *Astronomy Letters*, 23, 458
- Smith N., 2008, in F. Bresolin, P. A. Crowther, & J. Puls ed., *IAU Symposium Vol. 250 of IAU Symposium, Episodic Mass Loss and Pre-SN Circumstellar Envelopes*. pp 193–200
- Smith N., Conti P. S., 2008, *Astrophys. J.*, 679, 1467
- Smith N., Owocki S. P., 2006, *Astrophys. J.*, 645, L45
- Spiller F., 1992, PhD thesis, PhD Thesis, Landessternwarte Heidelberg/Königstuhl (1992).
- Sterken C., van Genderen A. M., Plummer A., Jones A. F., 2008, *Astronom. and Astrophys.*, 484, 463
- Valeev A. F., Sholukhova O., Fabrika S., 2009, *Monthly Notices Roy. Astronom. Soc.*, 396, L21
- Viotti R. F., Galleti S., Gualandi R., Montagni F., Polcaro V. F., Rossi C., Norci L., 2007, *Astronom. and Astrophys.*, 464, L53
- Viotti R. F., Rossi C., Polcaro V. F., Montagni F., Gualandi R., Norci L., 2006, *Astronom. and Astrophys.*, 458, 225
- Allen K. U., 1977, *Astrophysical parameters*. Mir

Table 1: LBV candidates with $(B - V) < 0^m35$. The columns give (in this order): the number of the object and its coordinates adopted from [Massey et al. (2006)]; our measured V -band magnitude and $(B - V)$ color index; the excess “s” of the $H\alpha$ -line flux above main sequence in the units of σ , and R, the object’s size $R_{0.9}$ averaged over four broad-band filters in arcseconds. The last column gives the results of cross-identification with the catalogs of emission-line objects ([Massey et al. (2007)] (M) and [Fabrika et al. (1997)] (SFZ)); variable stars [Hartman et al. (2006)] (HBS), and ultraviolet sources [Massey et al. (1996)] (UIT). If the object has a comment in catalog [Massey et al. (2006)] we repeat this comment here in the “m(comment)” format. The full version of the table is available from <http://jet.sao.ru/~azamat/LBVsearch/blue.dat>.

N	α	δ	V	$B - V$	s	R''	comment
1	2	3	4	5	6	7	8
000029	01:31:48.14	30:32:06.9	17.61	-1.10	2.04	1.18	
001429	01:32:27.81	30:21:46.8	18.40	0.32	3.09	0.95	
001705	01:32:29.08	30:34:04.2	17.71	0.30	1.73	2.23	SFZ515, HBS260273
003562	01:32:34.31	30:38:17.3	13.58	-0.21	2.41	1.1	
003935	01:32:35.25	30:30:17.6	18.08	0.04	4.69	1.98	HBS250024, M(hot LBV cand)
004926	01:32:37.72	30:40:05.6	17.48	-0.03	3.83	0.93	SFZ005, UIT003, m(Ofpe/WN9_M33WR2), M
005705	01:32:39.64	30:24:51.9	18.30	-0.09	4.24	2.15	M
006389	01:32:41.30	30:22:31.2	18.10	-0.03	3.9	1.32	HBS340115, M(HII)
008043	01:32:44.62	30:34:59.5	18.14	-0.15	9.21	1.23	HBS250385, M
008581	01:32:45.68	30:39:06.9	18.19	-0.14	11.35	0.82	HBS250451
008632	01:32:45.75	30:38:55.8	16.88	-0.04	4.89	1.4	m(WN_M33WR6)
009925	01:32:48.26	30:39:50.4	17.22	0.09	4.82	2.48	SFZ517, M
012779	01:32:52.95	30:34:50.3	18.10	0.07	1.18	1.18	
013846	01:32:54.37	30:30:50.6	17.88	0.24	1.78	1.07	
014939	01:32:55.68	30:35:34.7	17.65	0.04	1.64	1.15	SFZ022,m(B5Ia_ob21-40)
015651	01:32:56.47	30:35:30.9	18.53	-0.04	1.26	1.73	HBS250999
017442	01:32:58.71	30:31:52.9	17.96	0.07	1.05	1.05	HBS251139
018246	01:32:59.74	30:38:54.8	17.77	0.14	1.01	0.88	SF _x xZ033, M(HII?)
019512	01:33:01.24	30:30:51.3	18.30	0.22	3.59	1.05	M(HII 2)
021012	01:33:03.09	30:31:01.8	17.16	0.09	3.16	1.18	SFZ041, M(HII)
021189	01:33:03.31	30:11:21.8	18.20	-0.07	1.77	1.25	M
021331	01:33:03.50	30:33:23.1	18.39	-0.13	4.0	2.0	SFZ042, HBS251493,M
024824	01:33:07.60	30:42:59.0	16.76	0.34	1.44	1.85	SFZ049
024835	01:33:07.61	30:42:43.0	18.41	-0.14	2.44	1.23	M
025221	01:33:08.04	30:46:12.8	12.98	0.08	1.09	1.65	
025981	01:33:08.99	30:29:56.3	17.53	0.14	3.68	1.55	m(B8Iacomp_ob127-15),M
026091	01:33:09.14	30:49:54.5	18.24	-0.01	2.92	0.95	SFZ052, HBS150200, m(Ofpe/WN9_M33WR22,UIT045),M
027321	01:33:10.43	30:38:49.4	17.85	0.10	1.17	1.32	M
028115	01:33:11.25	30:45:15.4	15.26	0.10	10.04	3.92	M, UIT049, m(BI+neb)
028158	01:33:11.30	30:29:33.5	18.18	0.18	5.86	3.92	HBS240638
028322	01:33:11.45	30:29:51.3	17.12	0.06	3.25	2.2	M(HII)
028576	01:33:11.70	30:22:58.9	17.75	0.28	2.42	1.43	
028741	01:33:11.85	30:38:52.7	16.59	-0.01	2.06	1.25	
028771	01:33:11.88	30:38:53.5	16.42	0.00	2.77	1.57	m(WNL_M33WR25=MC17)
029660	01:33:12.81	30:30:12.6	17.48	0.17	1.96	1.07	HBS240772,M
030009	01:33:13.17	31:04:59.3	18.20	0.08	1.01	0.95	
031983	01:33:15.21	30:37:27.2	18.36	0.15	1.61	1.27	HBS241026
032127	01:33:15.34	30:37:22.6	17.13	0.34	1.59	1.77	
032629	01:33:15.82	30:56:44.8	16.51	-0.00	2.76	1.57	m(WN4.5+neb_M33WR33=MC23),M
033347	01:33:16.50	30:32:12.1	17.09	0.26	1.96	1.4	SFZ080, M(late A I/early F I)
033824	01:33:16.92	30:23:07.3	18.49	-0.00	1.59	1.38	SFZ084
037649	01:33:20.58	30:31:42.4	18.61	0.10	1.21	1.15	
045716	01:33:27.26	30:39:09.1	18.04	-0.12	4.43	1.27	HBS242552,m(Ofpe/WN9_M33WR39=MJC7),M
045922	01:33:27.41	30:31:31.7	18.38	-0.13	1.13	2.2	SFZ107,HBS242580,M
049612	01:33:29.88	30:31:47.3	17.88	0.01	13.17	1.27	M,UIT113,m(O+neb)

Table 1: (Contd.)

1	2	3	4	5	6	7	8
051296	01:33:30.99	30:36:52.5	18.37	0.22	1.65	1.23	SFZ119,HBS243138
053273	01:33:32.23	30:41:31.2	18.35	-0.15	5.95	2.3	M
054233	01:33:32.82	30:41:46.0	18.17	-0.19	3.52	1.27	m(WNL_M33WR42=AM3),M
054460	01:33:32.97	30:41:36.1	18.27	-0.15	4.91	1.05	m(WNL_M33WR43=AM4),M
054488	01:33:32.98	30:33:44.2	18.53	0.16	3.07	1.35	HBS243502
054767	01:33:33.13	30:35:06.3	17.72	-0.01	1.06	1.07	SFZ124,m(B8LR93-8),M
056807	01:33:34.27	30:41:36.7	16.54	0.07	12.37	2.08	M(WNL in HII)
056847	01:33:34.29	30:34:00.1	17.86	0.13	1.88	1.35	M(HII)
057017	01:33:34.39	30:32:08.4	18.20	-0.02	9.75	1.35	M(HII)
058382	01:33:35.14	30:36:00.4	16.67	0.12	2.64	1.3	m(LBV_VarC),M
058864	01:33:35.40	30:35:54.7	18.66	0.07	2.88	2.15	
060182	01:33:36.15	30:50:37.2	18.07	-0.12	1.44	1.57	UIT138,m(O6.5II),M
060689	01:33:36.42	30:35:30.9	18.03	0.05	1.11	1.27	SFZ141,HBS230123
060906	01:33:36.54	30:20:58.2	18.38	0.03	1.39	1.38	HBS320012,M
062775	01:33:37.58	30:28:04.7	18.15	0.16	1.27	2.27	
063555	01:33:38.01	30:31:48.6	18.06	0.07	2.24	2.12	SFZ149,HBS230517,M
065919	01:33:39.24	30:20:22.5	18.01	0.09	1.28	1.4	HBS320142
065935	01:33:39.25	30:43:03.6	18.63	-0.14	1.42	1.1	HBS140447,M
066011	01:33:39.28	30:20:53.6	18.10	-0.09	1.35	1.2	HBS320143,M
066512	01:33:39.52	30:45:40.5	17.31	0.11	7.83	4.42	SFZ163,m(MB0.5Ia+WNE_M33WR57),UIT154,M(P Cyg LBV cand)
069329	01:33:40.82	30:31:32.6	17.70	0.02	2.58	2.02	SFZ186,HBS231250,M
069374	01:33:40.84	30:38:22.5	18.17	0.18	1.22	1.52	HBS231309
070474	01:33:41.33	30:32:12.6	18.41	-0.00	2.19	1.07	SFZ191,m(O8:Ifob10-3),M
071501	01:33:41.80	30:21:10.7	18.03	0.14	3.13	2.45	HBS320276
072150	01:33:42.08	30:42:00.3	18.37	0.02	3.82	1.25	HBS140882,M
073722	01:33:42.78	30:32:56.3	18.12	-0.04	6.9	1.32	SFZ207,M
074495	01:33:43.10	30:39:04.5	18.05	-1.07	2.57	1.02	
074593	01:33:43.14	30:39:07.6	16.43	0.02	1.49	2.05	
075005	01:33:43.31	30:35:33.8	17.65	0.02	1.1	1.07	
075058	01:33:43.34	30:35:34.1	17.65	0.02	1.1	1.07	m(WN4.5+O6-9_M33WR75=UIT177)
076123	01:33:43.82	30:32:10.2	17.55	0.00	2.22	1.75	
076579	01:33:44.02	30:33:18.2	18.53	-0.10	2.14	1.38	M
076951	01:33:44.18	30:31:24.0	18.43	-0.08	1.49	1.32	SFZ217,M
077511	01:33:44.43	30:38:43.9	17.94	0.05	2.21	1.32	SFZ219,M
077826	01:33:44.56	30:32:01.3	18.36	0.00	8.58	1.98	SFZ221,M(HII)
078046	01:33:44.65	30:35:59.2	17.34	-0.02	2.15	1.23	m(B1.5Ia+_W91-258),M
078106	01:33:44.68	30:44:36.7	18.19	-0.03	10.65	1.38	m(WN8_M33WR77=OB66-25),M
078287	01:33:44.75	30:44:44.5	18.45	0.26	4.54	1.12	M
078412	01:33:44.79	30:44:32.4	18.23	0.07	8.78	1.38	HBS141343,M,m(OB+neb.ob66-28s),M(HII)
078458	01:33:44.81	30:32:17.8	18.12	-0.04	2.49	1.45	SFZ222, HBS232168,M
078579	01:33:44.87	30:32:11.0	18.77	-0.08	1.98	1.45	
078781	01:33:44.97	30:36:16.9	17.56	-0.08	2.08	1.3	M
079431	01:33:45.25	30:36:26.6	17.75	-0.08	3.73	1.23	M(HII),m(BI_W91-245)
080679	01:33:45.86	30:44:44.5	17.82	0.26	3.84	1.82	
082991	01:33:46.96	30:36:42.8	18.16	0.24	1.54	1.05	
083098	01:33:47.01	30:46:17.5	13.46	0.18	1.37	1.1	
083744	01:33:47.33	30:33:06.8	17.94	0.02	2.96	1.23	HBS232867,M(HII)
084795	01:33:47.82	30:43:24.9	17.72	0.10	1.08	3.17	SFZ237, HBS141903
085197	01:33:48.03	30:33:04.8	17.53	0.03	10.97	3.83	m(HII),UIT205
087513	01:33:49.22	30:38:09.3	16.29	0.03	7.44	1.18	M
087530	01:33:49.23	30:38:09.1	16.29	0.03	7.44	1.18	SFZ246, m(LBV_VarB)
089263	01:33:50.12	30:41:26.6	16.60	0.20	8.47	1.25	SFZ256,m(LBVcand),UIT212,M(LBVcand)
091640	01:33:51.42	30:40:00.7	18.39	0.17	2.29	1.3	M
091701	01:33:51.46	30:40:57.0	17.36	0.09	1.9	1.48	M(P Cyg LBV cand)
091715	01:33:51.47	30:38:48.7	18.13	0.01	1.25	1.1	SFZ268,M
092302	01:33:51.80	30:38:49.0	18.24	-0.14	2.99	1.35	SFZ271,M
092768	01:33:52.07	30:52:50.7	18.22	-0.08	1.51	1.3	
092935	01:33:52.16	30:33:33.5	18.00	0.16	2.28	1.65	HBS234175,M
092983	01:33:52.19	30:36:36.6	17.92	0.25	2.55	1.27	M(HII)

Table 1: (Contd.)

1	2	3	4	5	6	7	8
093303	01:33:52.39	30:39:20.9	16.85	-0.10	7.85	1.38	M(HII),m(OB+neb),UIT229
093351	01:33:52.42	30:39:09.6	16.20	0.24	1.48	1.32	new LBV [Valeev et al. (2009),M
093765	01:33:52.66	30:39:13.9	17.36	-0.05	3.75	1.6	m(B5:I_UIT231),M
094256	01:33:52.95	30:44:57.0	15.75	0.30	1.87	1.25	
094642	01:33:53.21	30:38:54.0	17.22	0.05	2.73	1.35	
095270	01:33:53.60	30:38:51.6	18.05	-0.12	5.96	1.35	HBS234654,m(Ofpe/WN9_M33WR103=MJX15),M
095281	01:33:53.61	30:38:43.0	18.47	0.25	4.81	1.35	
096035	01:33:54.10	30:33:09.7	17.09	0.07	10.79	1.98	m(O6-8If),UIT240
096860	01:33:54.64	30:33:08.2	17.71	0.06	2.86	1.52	
097162	01:33:54.84	30:32:48.9	18.48	-0.06	3.41	1.32	SFZ294,HBS234917,M
097751	01:33:55.21	30:34:29.9	17.16	0.03	1.92	2.38	m(B5Ia_ob4-4),M
098246	01:33:55.51	30:45:26.8	17.93	0.01	3.57	1.18	M(HII)
098632	01:33:55.75	30:45:30.1	18.44	-0.18	3.25	0.93	M
098810	01:33:55.87	30:45:28.4	17.32	-0.23	1.54	0.97	M(WNL in HII)
100400	01:33:56.85	30:34:29.7	17.81	-0.16	1.21	2.9	
100647	01:33:57.00	30:38:26.4	17.61	-0.15	1.61	2.85	SFZ301,M
101408	01:33:57.45	30:32:27.6	18.26	0.08	3.33	2.12	
101826	01:33:57.69	30:37:30.7	13.55	0.27	1.67	1.1	
101897	01:33:57.73	30:17:14.2	17.11	0.01	1.11	3.35	M(cool LBV cand)
101914	01:33:57.74	30:37:31.0	13.56	0.26	1.74	1.1	
102105	01:33:57.85	30:33:38.4	17.71	0.07	1.32	1.27	m(B2:I_B467)
102367	01:33:58.00	30:41:22.3	15.90	0.23	1.49	1.12	
102526	01:33:58.08	30:33:28.6	17.76	0.12	1.5	1.55	
103164	01:33:58.43	30:33:01.6	18.06	0.28	1.48	1.27	
103667	01:33:58.69	30:35:26.5	16.47	-0.07	2.6	1.52	m(B1Ia+WNE_M33WR115=OB2-4),M
104242	01:33:59.01	30:33:53.9	17.35	-0.02	1.46	1.4	M(B8I in HII),UIT278
104285	01:33:59.03	30:33:56.7	18.42	0.05	2.41	1.1	UIT269
104432	01:33:59.11	30:34:37.2	17.88	0.04	5.84	1.57	star in HII
104958	01:33:59.40	30:23:11.0	16.95	0.03	1.28	2.12	m(A0Ia_IFM-B1330),M(HII)
105428	01:33:59.67	30:33:33.1	18.07	0.12	3.07	1.55	HBS236226,M
105786	01:33:59.88	30:33:54.9	16.06	0.01	6.53	4.55	
105799	01:33:59.89	30:34:27.2	17.91	-0.11	5.14	1.6	m(B_ob4-39),M
106177	01:34:00.10	30:46:15.0	17.52	0.17	1.1	3.25	
106653	01:34:00.41	30:37:18.6	18.36	0.14	1.35	1.1	SFZ328,HBS236446
107707	01:34:01.05	30:36:34.7	18.12	0.12	2.63	1.2	
107775	01:34:01.08	30:36:19.6	17.35	0.05	4.73	2.62	UIT280,HBS236592,M
108708	01:34:01.68	30:37:20.0	18.40	-0.08	5.55	1.25	SFZ337,M(HII)
109058	01:34:01.92	30:38:19.3	17.84	-0.10	3.05	1.25	M
109156	01:34:01.99	30:38:53.8	17.43	0.04	2.88	2.27	M
109457	01:34:02.21	30:38:50.3	18.12	-0.06	5.6	1.38	M
109749	01:34:02.43	30:31:03.5	18.43	-0.02	2.26	1.3	SFZ349,HBS236868,M
115127	01:34:06.63	30:41:47.8	15.95	0.07	7.25	2.33	m(LBVcand),UIT301,M
115225	01:34:06.72	30:41:54.5	18.47	-0.18	7.74	1.4	M,m(EarlyO),UIT302,M
115375	01:34:06.83	30:47:22.4	17.46	0.32	14.86	1.57	
116383	01:34:07.70	30:45:22.9	18.46	0.28	1.73	1.25	SFZ369
116517	01:34:07.82	30:47:31.9	18.28	-0.02	2.95	1.15	HBS130240,M
117163	01:34:08.34	30:34:59.2	18.60	0.04	1.25	1.38	
119710	01:34:10.61	30:26:00.5	18.14	0.04	1.15	1.4	SFZ393,HBS220620,M
120082	01:34:10.93	30:34:37.6	16.22	0.12	3.31	1.1	SFZ394,M(hot LBV cand),var 83
120141	01:34:10.99	30:46:33.0	18.06	0.08	1.28	1.15	M
120145	01:34:10.99	30:24:55.0	13.09	0.12	2.21	1.73	
120530	01:34:11.33	30:36:28.0	18.63	0.10	4.12	1.55	SFZ543,HBS220732,M
120786	01:34:11.56	30:36:25.4	17.92	-0.00	4.07	2.17	HBS220767,M
120805	01:34:11.58	30:36:17.4	18.32	0.03	3.83	1.32	HBS220771,M
123649	01:34:14.21	30:53:55.2	18.32	0.10	2.77	2.62	SFZ405
123651	01:34:14.21	30:33:43.3	18.49	-0.03	8.86	1.2	HBS221094,M(HII)
124598	01:34:15.03	30:34:57.8	18.16	0.22	3.07	1.2	UIT330,SFZ550,HBS221214,M
124844	01:34:15.22	30:36:59.0	18.20	0.18	1.22	1.05	M
125294	01:34:15.56	30:37:12.6	15.82	0.03	10.02	3.52	

Table 1: (Contd.)

1	2	3	4	5	6	7	8
125342	01:34:15.61	30:41:11.0	18.59	-0.23	1.36	1.27	SFZ415,HBS131495,M
125850	01:34:16.05	30:33:44.2	16.87	0.02	4.01	1.18	UIT341,SFZ423,M
125867	01:34:16.07	30:36:42.1	18.09	-0.04	6.59	1.73	UIT339,SFZ422,HBS221349,M(P Cyg LBV cand)
125919	01:34:16.10	30:33:44.9	16.56	0.06	2.35	1.2	UIT341,SFZ423,m(LBVcand=B526),M
126188	01:34:16.35	30:37:12.3	18.17	-0.18	9.07	1.35	HBS221391,M,m(WN7_M33WR130),UIT343,HII
127134	01:34:17.20	30:33:39.2	17.61	-0.07	5.53	1.88	HBS221507,M
127502	01:34:17.56	30:33:39.3	17.72	-0.02	4.63	1.55	HBS221547,M
128224	01:34:18.36	30:38:36.9	18.12	-0.06	4.31	1.8	SFZ439,HBS221640,M
130073	01:34:20.68	30:48:59.9	17.97	0.09	1.76	1.62	
130074	01:34:20.68	30:39:42.7	18.14	0.01	1.83	0.9	SFZ450,HBS221885,M
130270	01:34:20.95	30:30:39.9	16.59	0.17	1.1	2.98	
132716	01:34:24.78	30:33:06.6	17.02	0.14	1.05	1.4	M(cool LBV cand)
134181	01:34:27.11	30:45:59.8	17.93	0.03	2.96	2.23	SFZ465,M
135855	01:34:29.71	30:53:12.0	18.16	0.29	1.37	1.18	
136261	01:34:30.29	30:40:39.8	17.82	-0.03	1.09	1.25	M(star in HII)
137219	01:34:31.97	30:46:49.8	18.56	-0.14	6.46	1.15	m(EarlyO),UIT361,M
139873	01:34:37.28	30:38:17.8	17.61	0.33	1.17	1.38	SFZ495
143582	01:34:49.96	30:29:21.3	13.86	0.32	1.24	0.85	
144082	01:34:52.76	30:28:12.2	13.44	0.14	1.81	1.02	
145023	01:34:59.39	30:42:01.2	18.43	-0.13	1.21	1.0	SFZ511HBS120967,m(O8Iaf_Lob88-7),M
145038	01:34:59.47	30:37:01.9	18.58	0.26	10.43	1.12	SFZ512,HBS210675,M(hot LBV cand)
146074	01:35:09.73	30:41:57.3	18.15	-0.22	5.09	1.1	HBS110031,M(Ofpe/WN9 Romano's Star)

Table 2: LBV candidates with $V > 16^m0$ and $0^m35 < B - V < 1^m2$. Designations are similar to those used in Table 1

N	α	δ	V	$B - V$	s	$R('')$	comment
1	2	3	4	5	6	7	8
002627	01:32:31.94	30:35:16.7	17.47	0.56	2.12	1.1	
006862	01:32:42.26	30:21:14.1	17.33	0.52	14.07	1.6	M(hot LBV)
009835	01:32:48.06	30:24:50.3	18.07	0.76	2.33	1.18	
021266	01:33:03.40	30:30:51.2	17.49	0.59	3.33	1.18	
031584	01:33:14.81	30:45:59.3	18.47	0.5	2.72	1.35	
045901	01:33:27.40	30:30:29.5	17.51	0.5	4.76	1.3	
052581	01:33:31.80	30:22:59.1	16.27	0.66	8.95	1.73	
057412	01:33:34.61	30:40:56.2	18.08	0.57	3.4	1.38	
058746	01:33:35.33	30:41:46.1	17.39	0.67	4.9	1.88	
061849	01:33:37.04	30:36:37.6	16.38	0.46	3.12	1.05	
073136	01:33:42.52	30:32:58.6	17.67	0.4	6.58	1.12	
075866	01:33:43.71	30:39:05.1	17.65	0.39	7.15	1.35	
077435	01:33:44.40	30:44:28.1	17.75	0.56	3.29	1.35	
077731	01:33:44.52	30:44:32.3	18.47	0.41	12.29	1.07	M(HII/OB+neb)
078101	01:33:44.67	30:36:11.4	17.63	1.18	2.14	1.15	
079224	01:33:45.15	30:36:20.1	16.59	0.4	2.01	1.12	
086876	01:33:48.89	30:21:48.6	17.73	0.74	2.56	1.32	
088927	01:33:49.94	30:29:28.8	18.23	0.78	2.38	1.38	M(HII)
104139	01:33:58.96	30:41:39.5	16.93	0.51	3.61	1.07	
115963	01:34:07.32	30:47:32.4	18.58	0.35	7.57	1.18	HBS130137,m(HII)
124485	01:34:14.93	30:34:36.4	18.49	0.77	2.02	1.93	HBS221202
124864	01:34:15.23	30:37:04.9	17.68	0.84	4.31	1.0	
125093	01:34:15.42	30:28:16.4	17.47	0.73	4.22	1.12	
141751	01:34:42.14	30:32:16.0	17.56	0.77	3.24	1.4	M(hot LBV cand?)
146528	01:35:23.21	31:06:38.5	17.63	0.75	10.41	1.35	